Electronic Supplementary Material (ESI) for Nanoscale.

Supporting Information

A First-Principles Study of Aggregation-Induced Intersystem Crossing in Fluorescent Dye Molecules

Li Yang,† Xijun Wang,† Guozhen Zhang, Xiaofeng Chen, Guoqing Zhang, Jun Jiang*

Hefei National Laboratory for Physical Sciences at the Microscale, Collaborative Innovation Center of Chemistry for Energy Materials, CAS Key Laboratory of Mechanical Behavior and Design of Materials (LMBD), School of Chemistry and Materials Science, University of Science and Technology of China, Hefei, Anhui 230026, P. R. China

**Corresponding author. E-mail: jiangj1@ustc.edu.cn*

†These authors contributed equally.

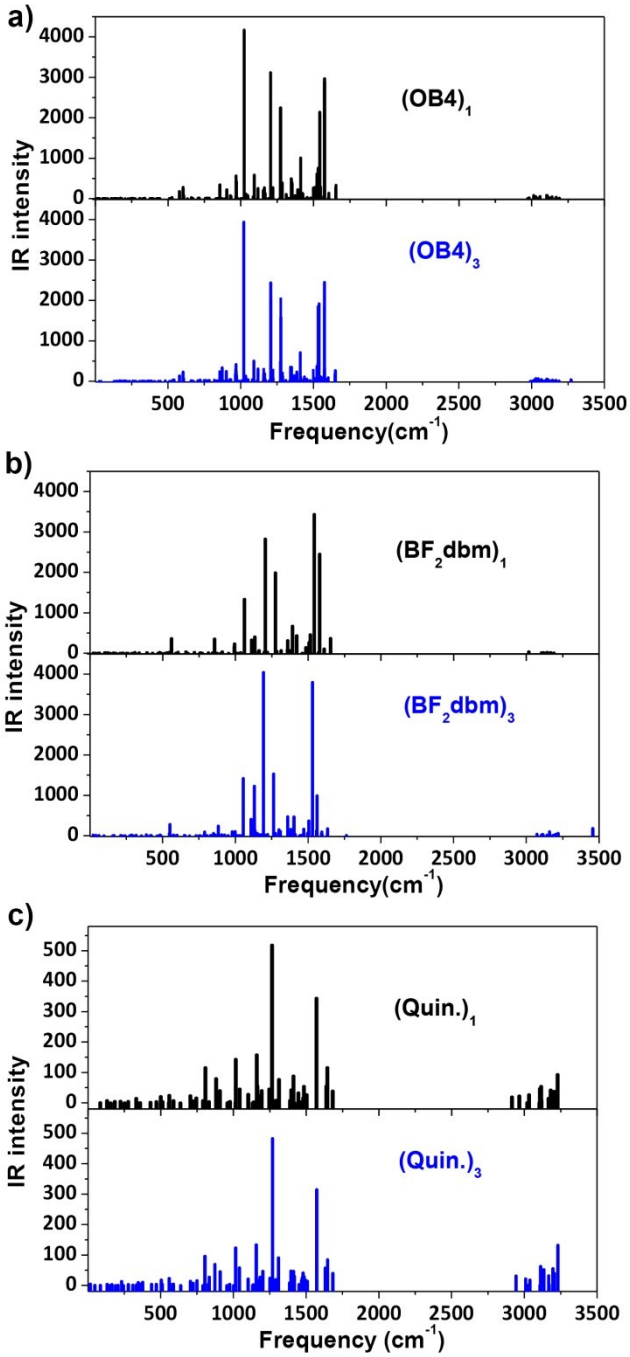

Figure S1. The distribution of vibrational intensities in the monomer and the sanwiched molecule of the trimer structure for OB4 (a), BF_2dbm (b) and quinoline derivative (c) molecules.

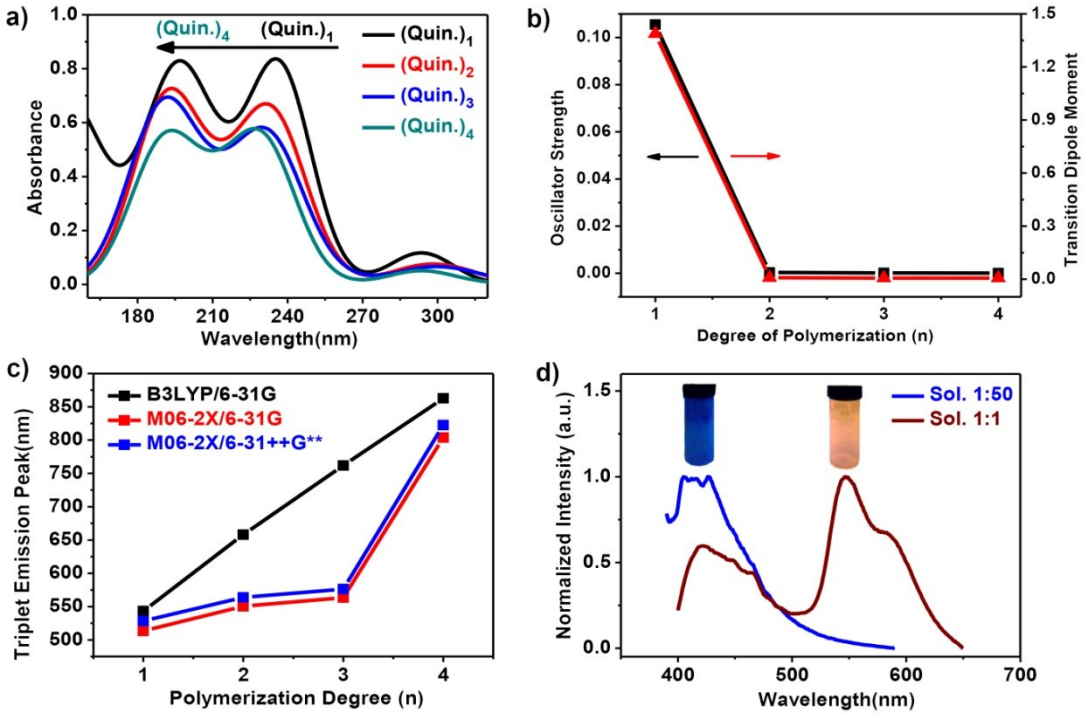

Figure S2. (a) The simulated photo-absorption spectra of the quinoline derivative monomer and aggregates. (b) The calculated emission oscillator strengths and transition dipole intensities for the $\mathbf{S_1}$ to $\mathbf{S_0}$ transition which produces fluorescence light. (c) The redshift of the phosphorescence emission ($\mathbf{T_1 \rightarrow S_0}$ transition) wavelength with the increase of aggregation degree for $(Quin.)_n$. (d) Experimentally measurements of quinoline derivatives in solution demonstrate that the fluorescence emission (~420 nm, ~ns) in low quinoline concentration did change to phosphoresce emission of (~550 nm, ~374μs) at high quinoline concentration.

The phosphorescence peak of $(Quin.)_n$ at ~543nm in experiment is consistent with that computed peaks of 543, 515 and 528nm at the B3LYP/6-31g, M06-2X/6-31g, M06-2X/6-31++g** level, respectively.

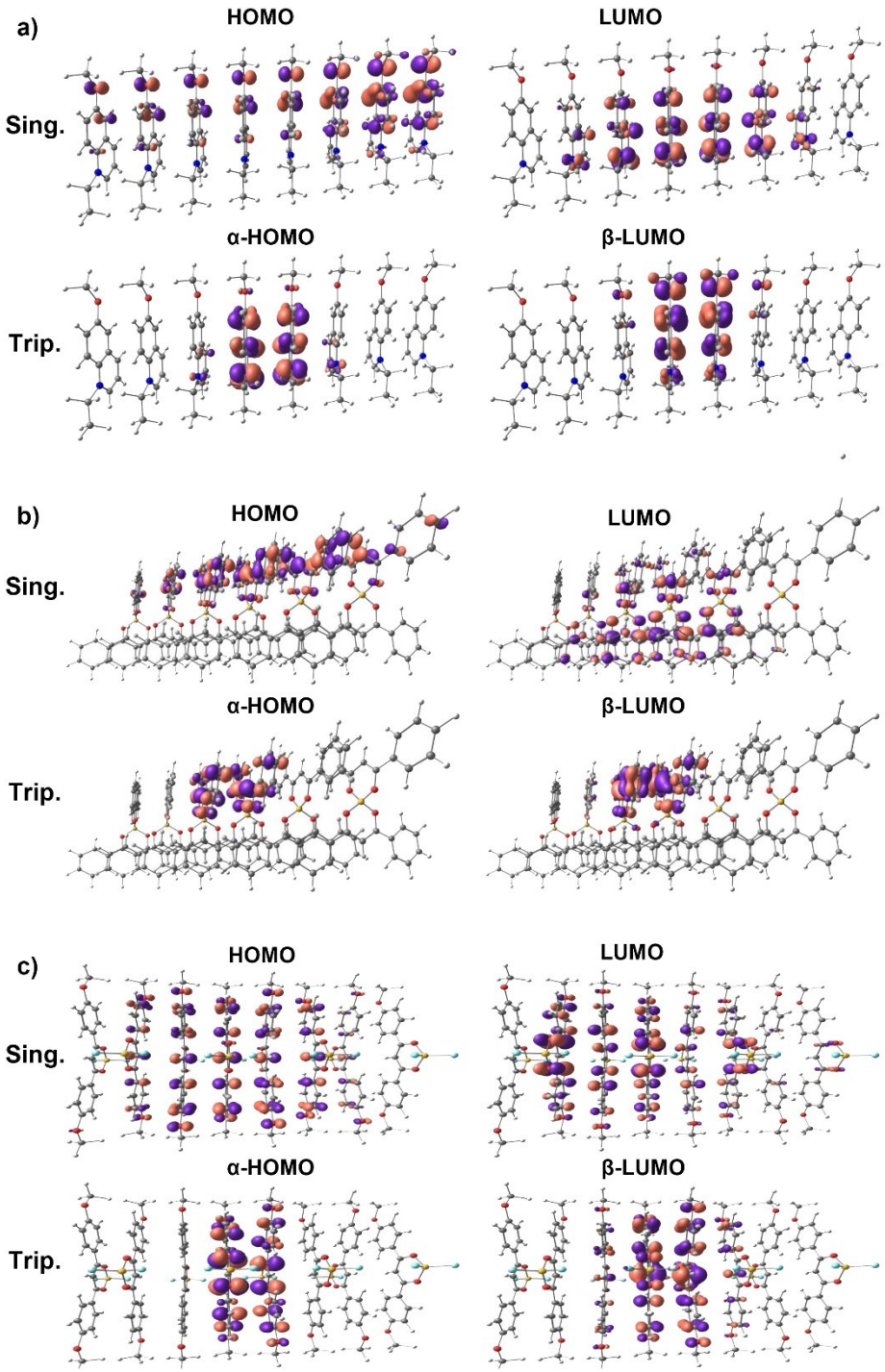

Figure S3. The simulated HOMO and LUMO wavefunction of $(Quin.)_8$ (a), $(OB4)_6$ (b), and $(BF_2dbm)_8$ (c) for the lowest-lying singlet ($\mathbf{S_1}$) and triplet ($\mathbf{T_1}$) excited states, respectively. Simulations are performed at the M06-2X /sto-6g level.

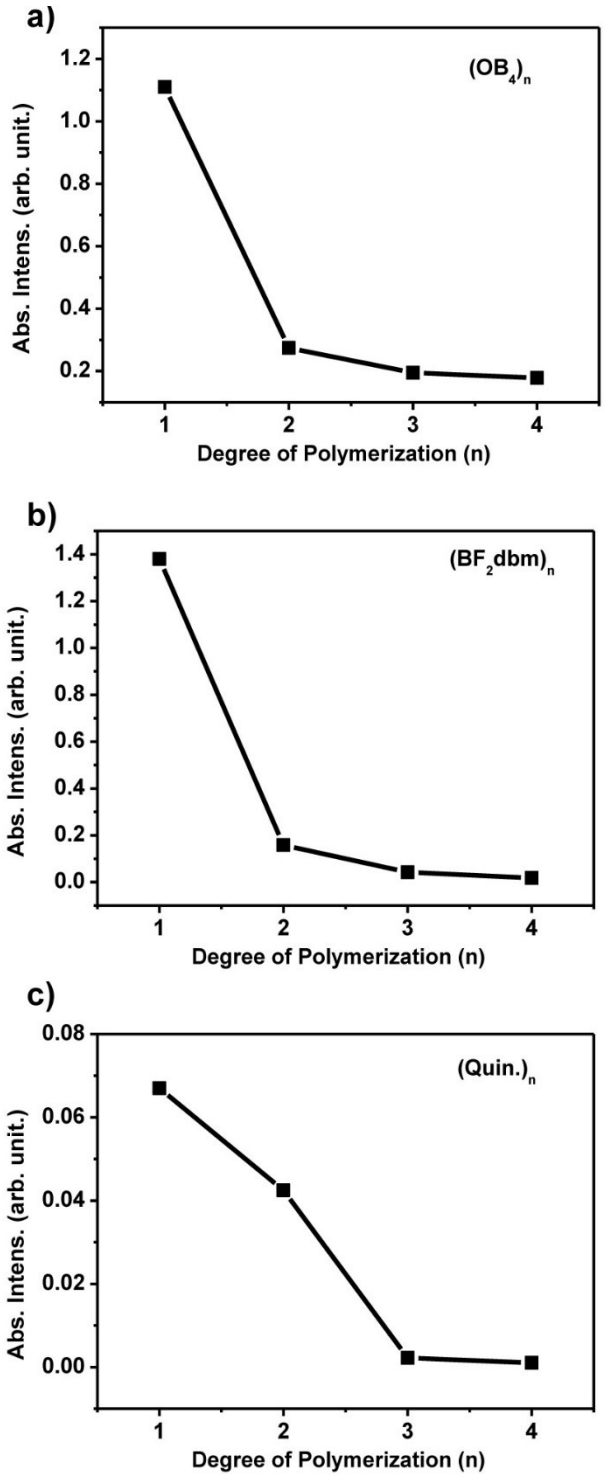

Figure S4. The absorbance intensity of the electronic transitions from the ground to the lowest excited states in $(Quin.)_n$ (a), $(OB4)_n$ (b), and $(BF_2dbm)_n$ (c) as the function of the number of aggregated molecules.

Evaluation of the intersystem crossing rate:

Other than the simple formula we proposed in the main text, we have also managed to evaluate the actual values of ISC rate for the monomer and dimer molecules (while the computations for bigger molecules are prohibitively expensive) with a formula based on the Fermi's golden rule and Condon approximation:[1]

$$k_{ISC}^{FC} = 2\pi \sum_{\alpha} \left| \left\langle \Psi_{Sa} \left| \mathrm{H}_{SO} \right| \Psi_{Tb}^{\alpha} \right\rangle \right|_{q0}^{2} \times \sum_{k} \left| \left\langle \{v_{aj}\} \middle| \{v_{bk}\} \right\rangle \right|^{2} \delta(E_{aj} - E_{bk}) = 2\pi \sum_{\alpha} \left| \left\langle \Psi_{Sa} \left| \mathrm{H}_{SO} \right| \Psi_{Tb}^{\alpha} \right\rangle \right|_{q0}^{2} \rho(E_{aj})$$

Here the spin-orbit coupling (SOC) factor is calculated as the wavefunction coupling between the lowest excited singlet state and several adjacent triplet states (with energy difference less than 1 $k_BT \approx 0.026$eV, 300K), as shown in Table S1. The vibronic factor is set to 1 to avoid very heavy computations. Applying the Plazcek approximation and Fourier transformation, the delta function is computed with $\delta(E_{aj} - E_{bk}) = \int_{-\infty}^{+\infty} e^{it(E_{aj} - E_{bk})} dt$, where the time interval goes through (-20000, 20000). We thus obtained the approximate ISC rates for the monomer and dimer structure of three proposed systems, as listed in Table S1. Obviously, despite of the small decrease of SOC from monomer to dimer, after considering the summation of ISC from the lowest excited singlet state to two adjacent triplet states, the substantial minimization of $\Delta E_{S\text{-}T}$ values eventually results in a significant increase of the total ISC rates. The same trend works for all three molecular systems, and should also be applied to the higher-ordered aggregates. These agree with our predictions based on the formula of $kISC \propto |\langle T\mathrm{i} \left| H\mathrm{SO} \right| S1\rangle|^2/(\Delta E_{S-T})^2$ as we described in the main text, and validate our proposed AI-ISC mechanism.

Table S1. The electronic spin-orbit coupling matrix elements, the integrals of the delta functions between the lowest excited singlet state and adjacent triplet ones together with the values of the ISC rate for the monomer and dimer quinoline (a), OB4 (b) and BF_2dbm (c) molecules.

a)

$(Quin.)_n$	$\langle \Psi_{S1} \lvert H_{SO} \rvert \Psi_{T1} \rangle$	$\langle \Psi_{S1} \lvert H_{SO} \rvert \Psi_{T2} \rangle$	$\delta(E_{S1}\text{-}E_{T1})$	$\delta(E_{S1}\text{-}E_{T2})$	k_{ISC}
Monomer	0.71	/	1.14	/	3.61
Dimer	0.20	0.47	1.50	2.91	4.34

b)

$(OB4)_n$	$\langle \Psi_{S1} \lvert H_{SO} \rvert \Psi_{T1} \rangle$	$\langle \Psi_{S1} \lvert H_{SO} \rvert \Psi_{T2} \rangle$	$\delta(E_{S1}\text{-}E_{T1})$	$\delta(E_{S1}\text{-}E_{T2})$	k_{ISC}
Monomer	0.41	/	3.63	/	3.98
Dimer	0.25	0.33	12.67	11.45	12.64

c)

$(BF_2dbm)_n$	$\langle \Psi_{S1} \lvert H_{SO} \rvert \Psi_{T1} \rangle$	$\langle \Psi_{S1} \lvert H_{SO} \rvert \Psi_{T2} \rangle$	$\delta(E_{S1}\text{-}E_{T1})$	$\delta(E_{S1}\text{-}E_{T2})$	k_{ISC}
Monomer	0.62	0.03	0.35	16.02	0.96
Dimer	0.08	0.18	5.51	7.59	1.78

[1] C. M. Marian, WIREs Comput. Mol, Sci. 2012, **2**, 187.